

Article ID: 169344
DOI: 10.5586/aa/169344

Publication History

Received: 2022-11-26
Accepted: 2023-03-10
Published: 2023-07-25

Handling Editor

Bożena Denisow; University of Life Sciences in Lublin, Poland;
<https://orcid.org/0000-0001-6718-7496>

Authors' Contributions

EP had a general idea for the present study and provided financing; BŁ & EP designed the analysis; BŁ & EW with the help of ES provided and collected plant material; EW & BŁ did the microscopic analysis; BŁ & ES wrote the manuscript

Funding

This research was financed by the Polish Ministry of Science and Higher Education grant nr 2 P06R 036 30 obtained by EP.

Competing Interests



BŁ - section editor at AA; EW, EP, ESz - no competing interests have been declared.

Copyright Notice

© The Author(s) 2023. This is an open access article distributed under the terms of the [Creative Commons Attribution License](#), which permits redistribution, commercial and noncommercial, provided that the article is properly cited.

ORIGINAL RESEARCH PAPER

Ultrastructure of receptive stigma and transmitting tissue at anthesis in two pear species

Barbara Łotocka ^{1*}, Emilia Wysokińska², Emilian Pitera², Ewa Szpadzik ²

¹Department of Botany, Institute of Biology, Warsaw University of Life Sciences – SGGW, Nowoursynowska 159, 02-776 Warszawa, Poland

²Department of Pomology and Horticultural Economics, Institute of Horticultural Sciences, Warsaw University of Life Sciences – SGGW, Nowoursynowska 159, 02-776 Warszawa, Poland

* To whom correspondence should be addressed. Email: kbot@sggw.edu.pl

Abstract

The ultrastructure of stigmatic and stylar secretory tissues was studied in one cultivar of *Pyrus communis* and six cultivars of *Pyrus pyrifolia* var. *culta* (the so-called Nashi pear) using standard light, scanning, and transmission electron microscopy methods. Although both tissues secreted an extracellular fluid necessary for the development of male gametophyte, they differed markedly in the ultrastructure of the extracellular matrix and in the distribution and ultrastructure of organelles. The difference was most evident in regard to the endoplasmic reticulum, which represented the rough, smooth, and vesicular type in stigmatic papillate epidermis and distal stigmatoid tissue cells and occurred mainly as the rough type in form of expanded cisternae filled with fine-fibrillar content in the transmitting tissue of the style.

Keywords

Asiatic pear; Japanese pear; leucoplast; papillae; pistil; secretory structures; style

1. Introduction

The East Asian cultivated pears, whose fruits bear market names Asiatic pear, Chinese pear, Korean pear, Japanese pear, Taiwan pear or sand pear, are classified variously as *Pyrus ussuriensis* Maxim, *P. bretschneideri* Rehder, *P. pyrifolia* (Burm. f.) Nakai, or as varieties within these species (Iketa et al., 2012). However, most cultivars express hybrid traits, and the relationship between cultivated forms and wild populations is not clear.

Traditionally, Asiatic pears were cultivated in Korea, China, and Japan, but for ca. 30 years this crop has been cultivated on a commercial scale within other suitable climatic zones, including Central Europe (Pitera et al., 2009). In addition to the market demand, this resulted mainly from their advantageously high yield, especially in young trees (Pitera & Odziemkowski, 2004). As is often the case of crop plants, studies on Asiatic pears were aimed mainly at their commercial or functional traits, specifically on self-incompatibility in the case of the species embryology (Claessen et al., 2019; Wang et al., 2010), with some gaps in fundamental studies.

The stigmatic epidermis and the stylar transmitting tract are pistil tissues essential for the completion of the male gametophyte development; additionally, processes determining the compatibility take place in these tissues (Lersten, 2008 and citations of original papers therein). The stigmas are diverse in terms of their shape and structure. Generally, they are covered by a modified epidermis. In contrast to the tabulate pavement cells of typical stem epidermis, stigmatic epidermal cells are anticlinally elongated into papillae with large intercellular spaces at their bases, which lead into the subtending stigma portions. Two types of stigmas are recognized. In dry

stigmas, pollen is deposited on a modified epidermis surface, which is “dry”, i.e., it is constituted by a papillar primary cell wall, a waxy cuticle and a proteinaceous pellicle (de Graaf et al., 2001; Edlund et al., 2004). In wet stigmas, papillae and the subtending stigmatic cells exude a notable amount of viscous fluid, which is an aqueous solution (or suspension) of lipids, polysaccharides, pigments, and proteins, the latter of surprising diversity (de Graaf et al., 2001; Rejón et al., 2013). In two species with wet stigma, *Lilium longiflorum* and *Olea europaea*, stigma exudate analyzed by proteomics contained enzymes for degradation of polysaccharides and lipids secreted by papillae into smaller compounds to be incorporated into the pollen tube or involved in the regulation pollen-tube growth through the selective degradation of tube-wall components (Rejón et al., 2013). Other secreted proteins were involved in pollen-tube adhesion or in the programmed cell death of the papillae cells, the latter in response to either compatible pollination or incompatible pollen rejection. The wet stigma lipidic cuticle seems permeable to water (Lolle et al., 1997; Pruitt et al., 2000), possibly due to cuticle ruptures, which facilitates rapid transport of water, nutrients, and regulatory molecules into the pollen grain after its deposition on the stigmatic fluid. The onset of secretion may be correlated with lysis or programmed cell death of some stigma cells (Crawford & Yanofsky, 2008; Heslop-Harrison et al., 1981).

Other secretory structures of the pistil are the stigmatoid tissue, also called the spongy zone (Raghavan, 1997) or glandular cells (Dumas et al., 1978); and the transmitting tissue (TT; Arber, 1937; Gotelli et al., 2017), the former located as an intermediary between the stigma papillate epidermis and the TT, and the latter - within the style. In species with an open style, TT consists of stylar canal secretory epidermis (Gotelli et al., 2017). In closed styles, a solid “core” of TT extends from the stigma-style boundary to the (base of) ovary. Transmitting tissue cells produce and secrete components of the extracellular matrix (ECM), which replaces the typical middle lamella and is a medium of multiple function in pollen tube recognition, guidance, and nutrition and in defense against pathogens (Gotelli et al., 2017). Differential programmed cell death, resulting in removing (or reducing) physical barriers for growing pollen tubes, may be involved in the development of functional TT (Crawford et al., 2007; Crawford & Yanofsky, 2008; Wang et al., 1996). Transmitting tissue cell death may be correlated with the onset of extracellular matrix (ECM) secretion but the causal relation between them is unclear.

In *Pyrus* spp., the syncarpous gynoecium (pistil) is composed of 2–5 carpels with fused ovaries (and adnate to the concave receptacle) (eFloras, 2008). In *P. communis*, the ovary is 5-locular, and 5 basally pubescent styles are typically formed. In Asiatic pears, the ovary is 5-locular (rarely 4-locular, but in some cultivars 6 carpels are observed in some flowers) with the same number of glabrous styles with punctate (=dot-like) stigmas. The development of stigmatic papillae of *P. communis* was followed by means of fluorescence microscopy in flowers emasculated at the balloon-bud stage and hand-pollinated at anthesis or after pollination delayed till the 10th day post-anthesis in 2-days intervals (Sanzol et al., 2003). The stigmatic secretion was first noticed between papillae in yet non-receptive stigmas, while the stigmatoid tissue intercellular spaces were still free of fluid; at this stage, the secreted fluid did not support pollen hydration. The stigmatoid tissue entered the secretory stage in the receptive stigmas, resulting in an increase in the stigmatic fluid volume and pollen hydration and germination. Pollination was associated with the loss of papilla turgidity, and the process was visible in the documentation ca. 24h post-pollination, when pollen tubes reached ca. 15% of the style length. Developmental asynchrony was discovered between the stigmas of the same pistil. The subcellular features of the stigmatic papillae were not analyzed in the cited study.

Apparently, every style guides pollen tubes to a separate ovary chamber in *Pyrus* spp. (eFloras, 2008) and *Malus communis* (Cresti et al., 1980), a species closely related to *Pyrus* spp.; however, in a cultivar of *Malus × domestica*, the individual TT strands of the free styles form a compitum in the basal (fused) part of the style (Sheffield et al., 2005), thus facilitating pollen tube growth redirection between carpels. The ultra-structure of TT was studied in Japanese pear ‘Nijuseiki’ (Nakanishi et al., 1991). The deposition of a fibrillar substance in the periplasmic space of TT cells, proliferation of

the rough endoplasmic reticulum (RER), and presence of large lipid “droplets” were indicated as the most characteristic features of the TT cells.

The stigma is adapted to pollen capture and hydration to allow pollen germination and subsequent entry of the pollen tube into the stylar transmitting tract (stylar canal epidermis or TT), which guides the tube towards ovules (Edlund et al., 2004). While these events take place, a complex signaling mechanism is operating at the interface of pollen structures and stylar secretory tissues to (1) block the development of foreign pollen or pollen expressing the same S alleles as pistil tissues; (2) block the invasion of pathogens *via* the transmitting tract. In recognition of the important role of the pistillar secretory tissues, this work was focused on the microscopic examination of two tissues essential for self-incompatibility and defense events, namely stigmatic epidermis and TT of the Asiatic pears style, with the respective tissues of *P. communis* as a background for comparison.

2. Material and methods

2.1. Light microscopy (LM) and transmission electron microscopy (TEM)

Pyrus caucasica-grafted cultivars of *Pyrus communis* L. var. *sativa* (Candolle) Candolle (‘Konferencja’) and Asiatic pear cultivars of either Japanese provenience (‘Chojuro’, ‘Shinseiki’, ‘Kosui’, and ‘Nijisseiki’) or Chinese provenience (‘Early Shu’ and ‘Shu Li’) were taken for LM and TEM examination. During anthesis, ten flowers with confirmed pistil receptivity, emasculated and isolated or left for free-pollination, were sampled from different trees of each cultivar, and one stigma and style were cut out from every flower. Since anthesis is a prolonged period in both species and lasts ca. 3–6 days depending on temperature, the stigma receptivity stage was determined (on a single style per flower) using a fast method proposed by McGee-Russell (1958), which consists in visualization of stigmatic free calcium ions by means of 5–10 min staining with 2% aqueous Alizarin Red S pH 4.1–4.3.

Samples were fixed, post-fixed, dehydrated, embedded in epoxy resin grade hard, and sectioned for LM or TEM according to a standard protocol, as described earlier (Łotocka & Osińska, 2010). Semi-thin (3–5 µm) sections were examined and documented using a light microscope Provis AX1 (Olympus) equipped with a dedicated digital camera. The images were saved as tiff files. Ultra-thin sections were examined using a transmission electron microscope (TEM) Morgagni 268 (FEI Company) at 80 kV. Digital images were saved as tiff files using a Morada (SIS) digital camera.

In the images chosen for this publication, the gamma level and/or contrast were adjusted with the respective tools of Adobe Photoshop CS6 (Adobe) software. The resulting images were prepared for publication using CorelDRAW®2020 (Corel Corporation) software.

2.2. Scanning electron microscopy (SEM)

For SEM observations carried out in the Analytical Centre of Warsaw University of Life Sciences-SGGW, the following samples were collected from selected cultivars only (‘Konferencja’, ‘Shinseiki’, and ‘Early Shu’):

1. balloon-stage flower buds,
2. flowers at anthesis, emasculated at the balloon-bud stage (stamens only removed), artificially pollinated or protected against pollination,
3. intact flowers at anthesis, after free pollination.

The non-coated stigmas were observed under low vacuum (ca. 0.89 Torr) using a scanning microscope Quanta 200 (FEI Company) operating at 20 kV. The images were saved as tiff files and prepared for publication as described above.

3. Results

In all the cultivars investigated, the anatomical or ultrastructural features of the stigma and TT were identical or very similar. Therefore, if not stated otherwise, the following description applies to all the cultivars of both pear species.

3.1. Secretory epidermis of the stigma

In the pear cultivars investigated in this work, the stigma was covered with modified epidermis (stigmatoïd tissue) consisting of anticlinally elongated unicellular papillae. In balloon-stage flower buds, the stigma surface was in the pre-secretory stage (Figure 1A). The papillae had already been differentiated and differently shaped between the 3 cultivars examined. The papillae were cylindrical and sometimes bent in ‘Konferencja’, (Figure 1A), apically swollen in ‘Shinseiki’ (Figure 1B), and bottle-shaped in ‘Early Shu’ (Figure 1C). At anthesis, the stigmas in the flowers of the 3 cultivars were either entirely covered by the secretion (Figure 1D) or by papillae tips protruding (Figure 1E). In the conditions of low-vacuum SEM observation, the evaporative drying of the ‘Shinseiki’ stigmatic secretion was markedly slower than in the two other cultivars, which suggests its higher viscosity or a different chemical composition of its cuticle. In emasculated flowers examined using SEM at anthesis, the secretion was often dried and the papillae were exposed (not shown). Stigmas with numerous pollen grains deposited, both after hand-pollination or open pollination, had a sparse secretion and their papillae were often collapsed, indicating their degradation.

When outer-whorl anthers completely folded back towards petals, stigmas became highly alizarin-positive (Figure 2A) due to the high content of free calcium. Therefore, based on findings reported by Bednarska (1989, 1991), they were considered to be

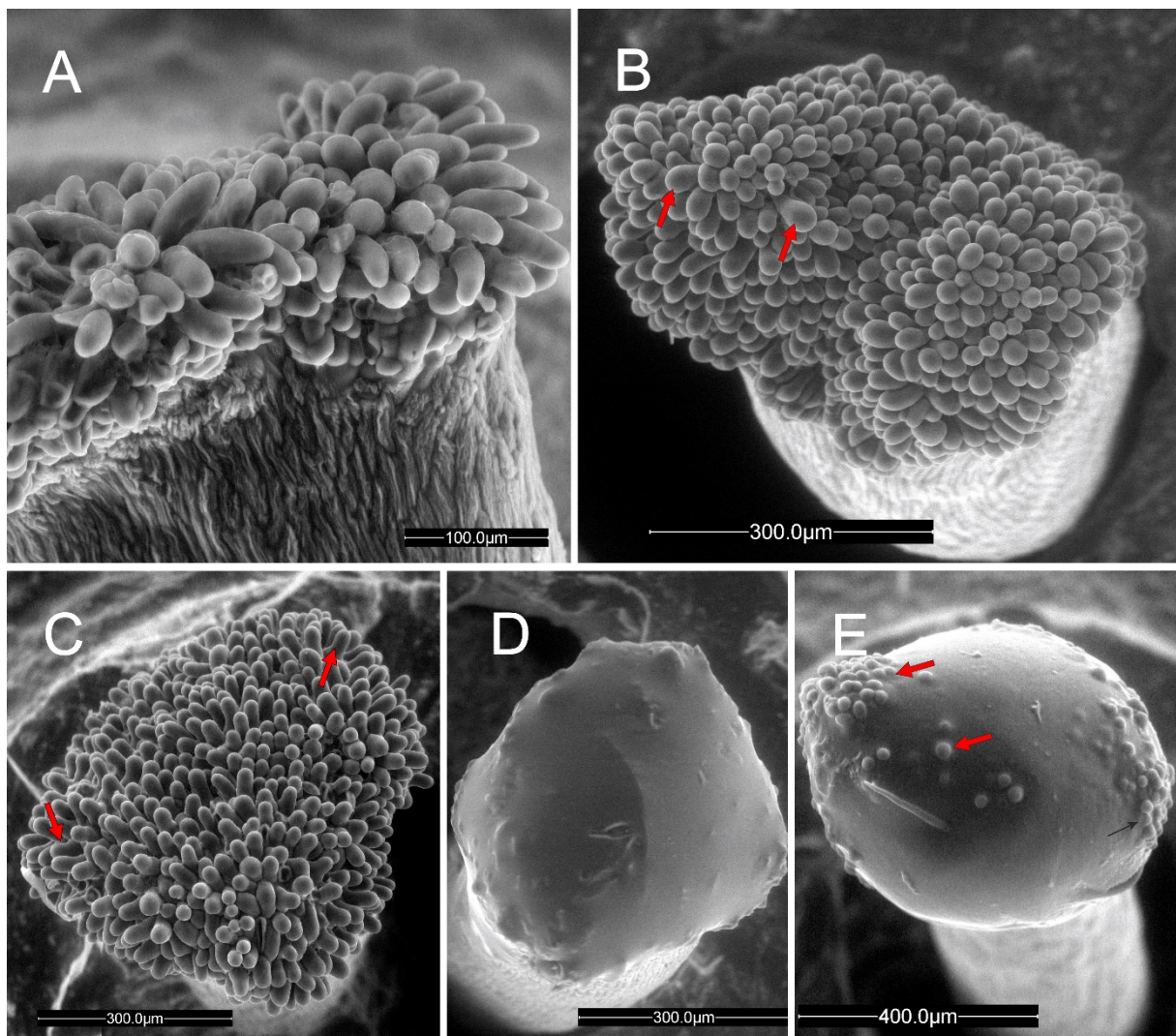


Figure 1 Unpollinated stigma, SEM. Papillae (arrows) exposed at the balloon stage (A–C, ‘Konferencja’, ‘Shinseiki’, ‘Early Shu’, respectively) and covered by a secretion at anthesis (D,E, ‘Shinseiki’). In (A), note the difference between stigmatic papillate epidermis and sub-stigmatic epidermal pavement cells; in E, note the protruding papillae apices.

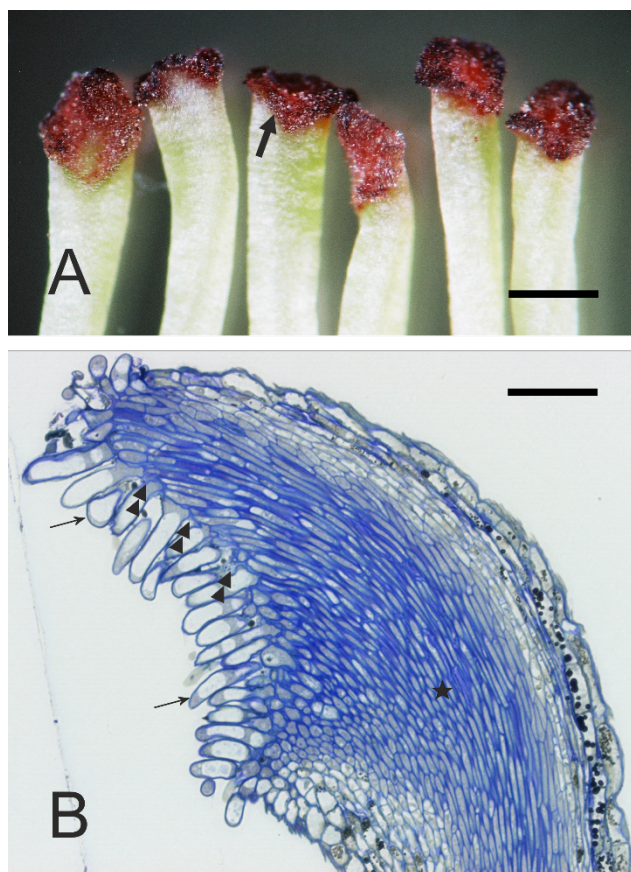


Figure 2 Stigma morphology and anatomy. (A) Dark staining of papillae (arrow) with Alizarin Red; ‘Shinseiki’, dissecting microscope. (B) Longitudinal section showing gaps (double arrowheads) between papillae (arrows) leading to the transmitting tissue (asterisk) of the style; ‘Konferencja’, LM. Scale bars 1 mm and 100 µm, respectively.

receptive, and stigmas from such flowers were sampled for sectioning. Their examination using LM or TEM revealed no differences in the anatomy or ultrastructure between the species or cultivars. Thus, the following description applies to all of them.

The stigmatic surface was diagonal in regard to the style axis and slightly concave (Figure 2B). The papillae were elongate, with a flat or irregular base. Numerous gaps between the papillae were continuous with intercellular spaces within stigmatic internal tissue. In pollinated stigmas, their entire surface or only their parts in contact with the pollen showed papillae in various stages of degradation, including final cell collapse. In receptive stigmas protected from pollination, ultrastructural polarization was evident in papillae. The basal (proximal) part was cytoplasm-rich, and the distal part was strongly vacuolated (Figure 3A). The cell nucleus was irregularly shaped or lobed and it was located in the proximal part, as were also numerous leucoplasts and mitochondria (Figure 3A, Figure 3B).

Papillary leucoplasts were variable as to their shape (irregular to cup-like), size (the small profiles may have represented stromules), and inner structure (Figure 4A–F), and their diversity was noticeable even between papillae of the same stigma. Their most characteristic and recurring feature was the presence of the peripheral reticulum, i.e., an extensive system of tubules or cisternae formed as a result of the invagination of envelope’s inner membrane into the stroma. Within the invagination lumen or in the stroma, inclusions were observed that differed in their electron density, amount, and shape. Papillary leucoplasts were evidently different from those in the pavement cells of the typical epidermis (i.e., non-secretory) just below the stigmatic papillate epidermis, as the latter leucoplasts were larger, rounded and contained single proteinaceous inclusion and numerous electron-dense plastoglobuli (Figure 4G, Figure 4H).

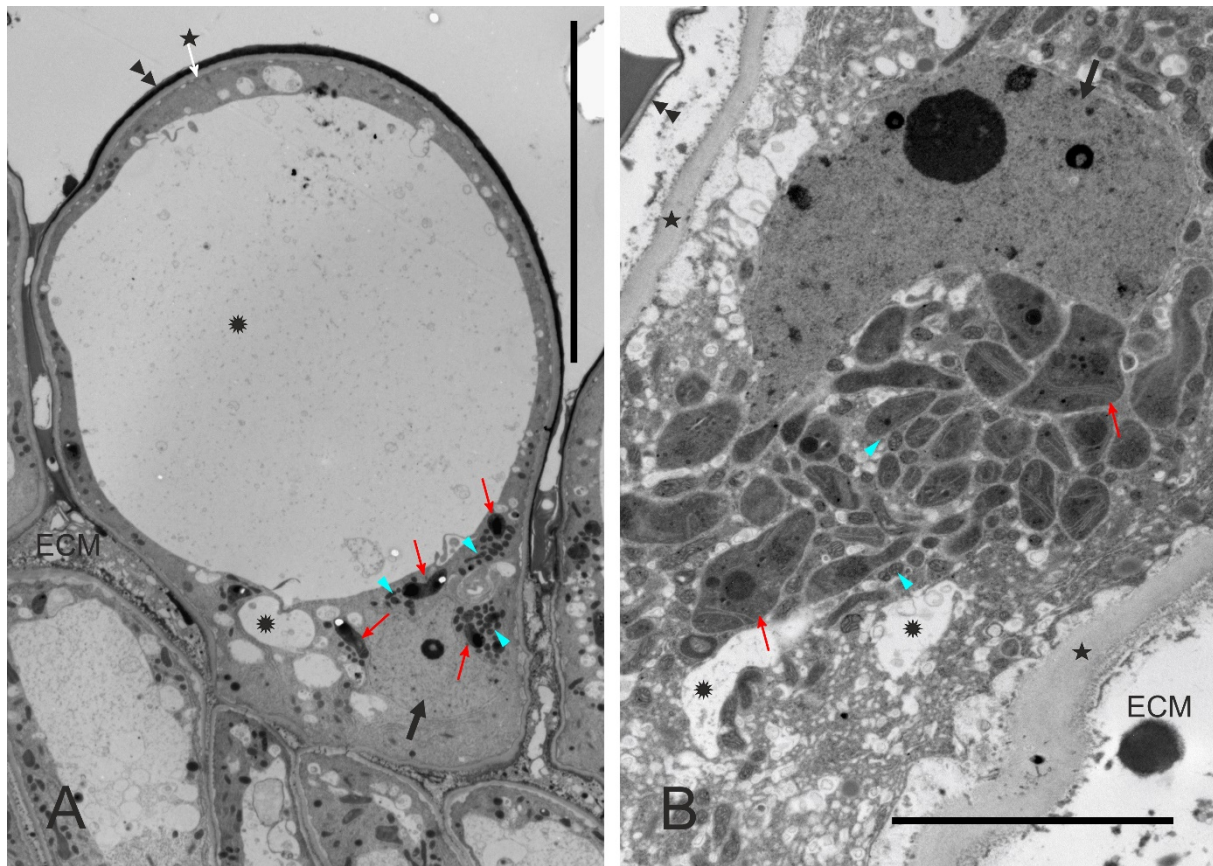


Figure 3 Ultrastructure of papillae at anthesis, unpollinated stigma, ‘Shu Li’ (A, papilla general view) and ‘Early Shu’ (B). The proximal part of the cell (B) is rich in cytoplasm. ECM – extracellular matrix; asterisks – cell walls; double arrowheads – cuticle; rosettes – vacuoles or vacuole-like vesicles; slim red arrows – leucoplasts; blue arrowheads – mitochondria; thick black arrows – cell nucleus. Scale bars 20 μm and 5 μm , respectively.

Additionally, the peripheral reticulum was usually very sparse in the leucoplasts of substigmatic epidermis.

Within the whole cytoplasm of papillae, the rough (RER), smooth (SER), and vesicular endoplasmic reticulum, vesicles, Golgi structures, lomasomes, small vacuoles, multivesicular bodies, membrane coils, and autophagosomes were abundant, and such proliferation of the membranous structures was consistent with the secretory function of papillae. In developmentally “younger” papillae (unpollinated receptive stigmas), RER cisternae were often observed in regular striated configurations (not shown). In “older” papillae, cytoplasmic domains rich in either RER or SER, with numerous Golgi bodies and vesicles were observed. The autophagosomes were routinely observed, also in papillae protected from pollen deposition (Figure 4A). The degradation of papillae was observed after pollination, and it proceeded probably by means of rapid lysis of the cell content after tonoplast breakdown, as suggested by the state of the papilla from a pollinated stigma shown in Figure 5.

The cell wall was thin in the papillae (Figure 5). In their proximal part, i.e. in contact with subtending stigmatoid tissue cells, the papillar cell wall had numerous plasmodesmata (Figure 6A). The free parts of the papillary cell wall (i.e. the distal one, not in touch with any other cell) were covered by an electron-dense cuticle. It adjoined the cell wall tightly in developmentally “younger” papillae. In such cells, also the plasma membrane was rather smooth. With the onset of secretory activity, the plasma membrane became sinuous in cross section, and “droplets” of secreted substance were visible first in the periplasmic space and next subcuticularly (Figure 6B). Successively, the cuticle separated from the cell wall, due to both the loosening of the wall outer face and the accumulation of the secretion. The secretion was also present on the outer surface of the cuticle, implying its putative discontinuity. The ultrastructure of the secretion suggests its mixed character, with domains rich in lipids (moderately

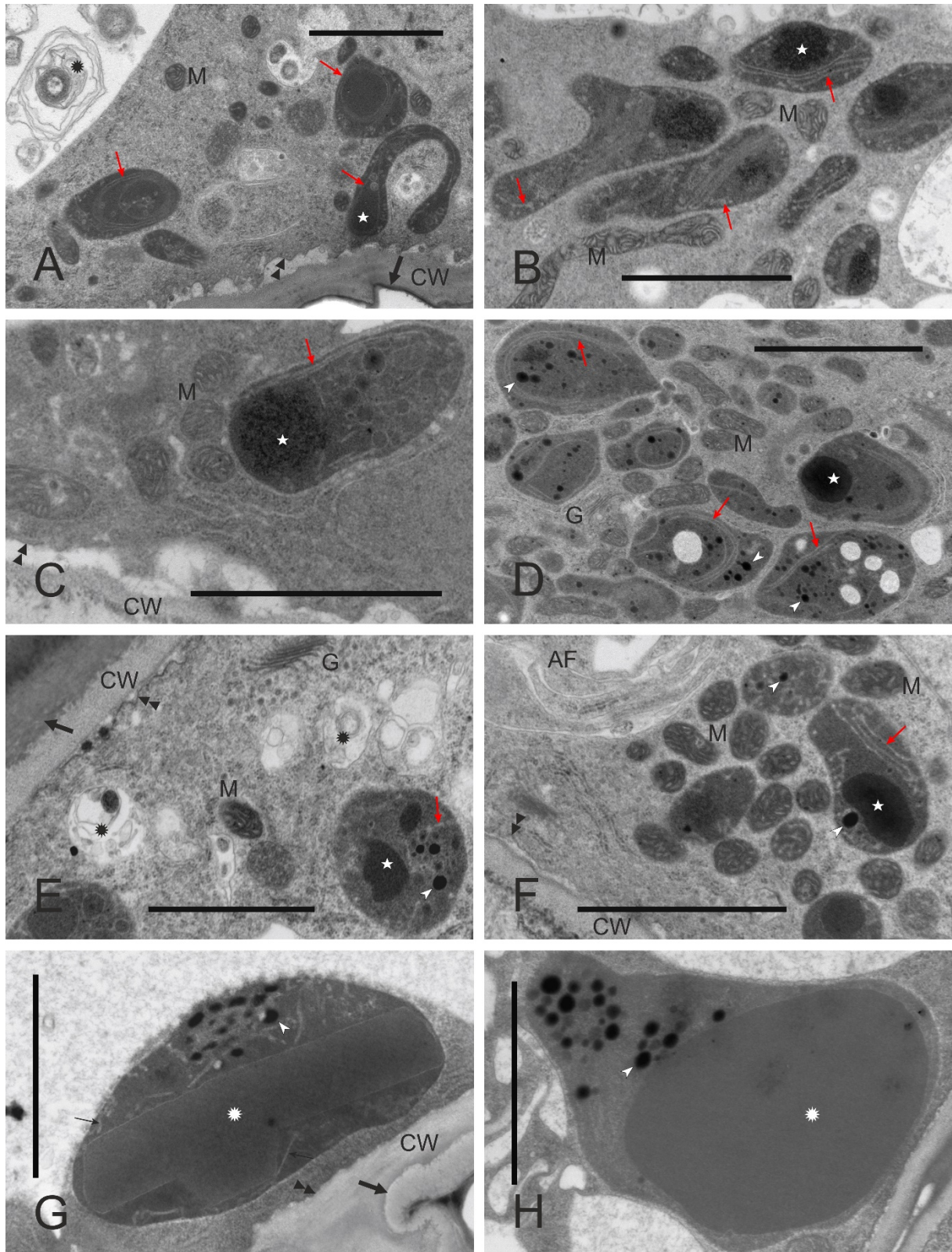


Figure 4 Diversity of leucoplast ultrastructure in unopened stigmatic papillae (A–F, ‘Konferencja’, ‘Chojuro’, ‘Nijisseiki’, ‘Early Shu’, ‘Shu Li’ and ‘Shu Li’, respectively) and in style epidermal cells just below the stigma (G,H, ‘Shinseiki’) at anthesis. AF – autophagosome; CW – cell walls; G – Golgi bodies; M – mitochondria; slim red arrows – extensive peripheral reticulum (i.e., system of envelope’s inner membrane invaginations); white asterisks – large electron-dense inclusions; arrowheads – plastoglobuli; white rosettes – proteinaceous inclusions; black rosettes – membrane coils in vacuoles; double arrowheads – plasma membrane; thick arrows – cuticle. Scale bars 2 μ m.

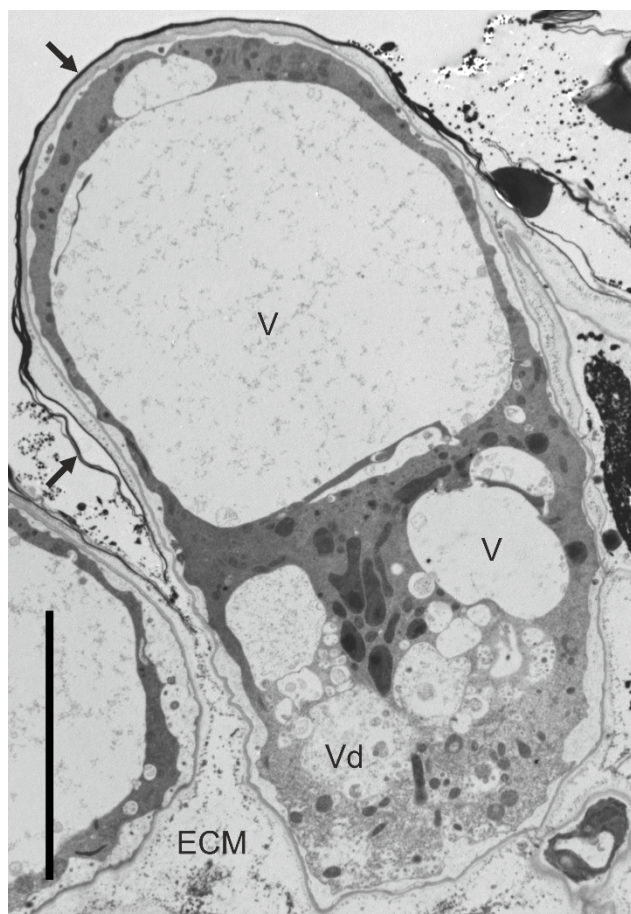


Figure 5 Ultrastructure of a papilla at the onset of lysis after pollination (the pollen grain is located beyond the image), ‘Chojuro’. ECM - extracellular matrix; V – vacuoles; Vd – vacuole with degraded tonoplast surrounded by electron-transparent cytoplasm; arrow – cuticle. Bar 10 μ m.

electron dense) or lipids and phenolics (electron opaque, [Figure 6C](#)). The latter accumulated in papilla-pollen grain contact areas before pollen germination (not shown).

The secretion filled intercellular spaces at the interface of papillae and the subtending cell layer of the stigmatoid tissue ([Figure 6C](#)). The secretion was heterogeneous, with a fine-fibrillar component and electron-dense fine globules.

3.2. Style and transmitting tissue

In cross-section, the styles were elliptic with a longitudinal shallow groove in every species and cultivar examined ([Figure 7](#)). The style was solid, i.e. with a central “core” of TT composed of elongated cells, rounded in cross-section. They were compactly arranged at the periphery of the TT strand and very loosely in its center. Using LM, TT was easy to distinguish from the surrounding chlorenchyma due to the low vacuolation and abundance of a deeply-staining intercellular matrix. The transmitting tissue strand was surrounded by poorly differentiated chlorenchyma with a few (3–8) vascular bundles. Although the bundles were not encircled with a bundle sheath, the boundary of the bundles and chlorenchyma was very distinct in the Chinese cultivars (‘Early Shu’, [Figure 7](#); and ‘Shu Li’), in contrast to the other cultivars. Numerous chlorenchyma cells had considerable amounts of electron-dense phenolic globules in their vacuoles. The uniseriate styler epidermis had a longitudinally ridged outer surface and a thick cuticle.

In every taxon examined, TT had similar ultrastructure. Cells at different developmental stages were observed in the same cross-section ([Figure 8A](#), details in [Figure 8B–F](#), [Figure 9A–B](#)): cells completing their differentiation (stage 1), mature cells

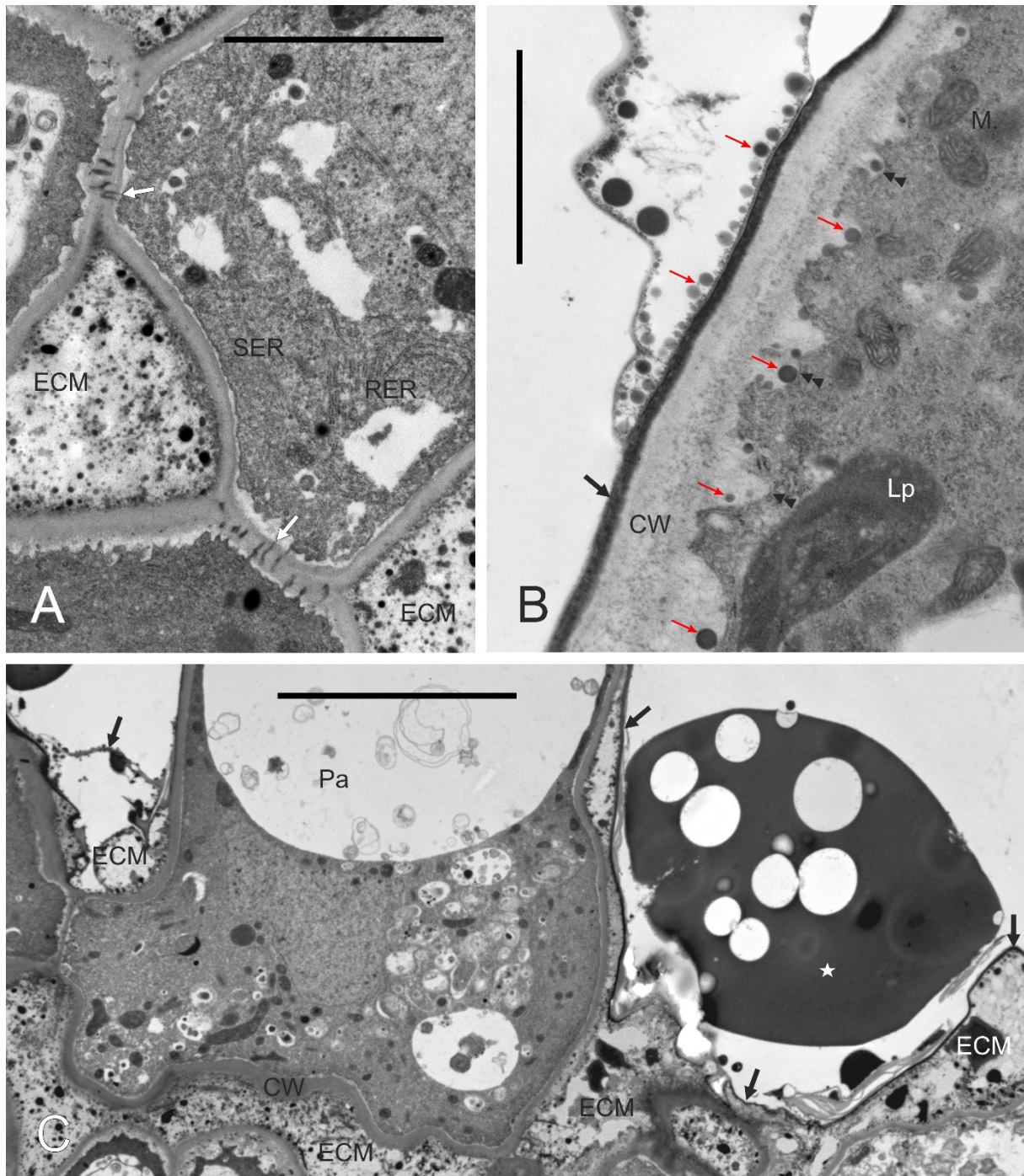


Figure 6 Ultrastructure of the papillar cell wall and extracellular secretion, 'Konferencia'. Extracellular matrix (ECM) present in intercellular spaces (A,C), between the cuticle and the papilla cell wall (C) or on the cuticle (B). CW – cell wall; Lp – leucoplast; M – mitochondria; Pa – papilla; RER – cytoplasmic domain rich in RER; SER – cytoplasmic domain rich in SER; white arrows – plasmodesmata; black arrows – cuticle; slim arrows – electron-dense globules secreted from the papilla; double arrowheads – plasma membrane; asterisk – heterogeneous secretion droplet. Scale bars 5 μ m, 2 μ m and 10 μ m, respectively.

(stage 2), and cells entering senescence (stage 3). They differed mainly in the RER ultrastructure and electron density of cytoplasm surrounding organelles. In stage 1 cells, the RER cisternae had a narrow lumen and the cytoplasm was electron dense (Figure 8B–F). In mature cells, the RER cisternae were much more widened with accumulated fine-fibrillar substance (Figure 8D–F). The ultrastructure of the cytoplasm changed in two contrasting ways in senescent TT cells (Figure 9A–B). It became dense in some cells but transparent to electrons in others, and the latter change coexisted with tonoplast fragmentation indicating lysis. In all senescent cells, widening of RER cisternae was evident. Independently on their developmental stage, the TT cells

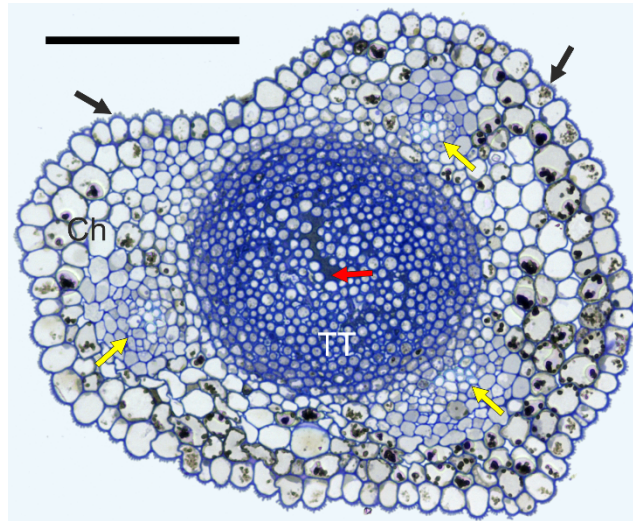


Figure 7 Anatomy of the style, 'Early Shu'. Ch – chlorenchyma; TT – transmitting tissue; black arrows – cuticular ridges on the epidermis; yellow arrows – vascular bundles; red arrow – extracellular matrix in transmitting tissue. Scale bar 100 μ m.

contained numerous active dictyosomes (Figure 8B, Figure 8D, Figure 9B) with abundance of associated vesicles indicative of an active exocytosis process. Various membranous structures were frequently present at the cell membrane and in the vacuoles.

In contrast to the poorly differentiated chloroplasts within stylar chlorenchyma, leucoplasts with electron-dense stroma, tubular membrane system (peripheral reticulum), and small starch grains were observed in TT cells (Figure 8B–C, Figure 8E). Within the peripheral reticulum, electron-dense substance was occasionally accumulated. The leucoplasts were diversely shaped. In more differentiated cells, they became cup-shaped. Lipid bodies, mitochondria, vacuoles, or dictyosomes were present in the cytoplasm filling the concavity of the leucoplasts, but usually RER cisterns occurred there (Figure 8C, Figure 8E). Often, small droplets similar to lipid bodies tightly adhered the outer surface of the leucoplast envelope (not shown), which suggests the participation of these plastids in their formation.

In TT cells, the plasma membrane had only slightly sinuous outline. On the outer surface of this membrane in stage 1 cells, deposits of substance with high electron density, ultrastructurally different from the cell wall, were observed (Figure 8B). In senescing cells, the space between the plasma membrane and the cell wall was gradually widened (Figure 9B).

The TT cells were interconnected with numerous plasmodesmata (not shown). These connections were abundant in transversal walls and locally numerous in places of contact of lateral walls. The ultrastructure of the outer surface of the TT cell wall in comparison with its inner surface suggests dispersion of its components into ECM (Figure 8D, Figure 8F), which completely filled the intercellular spaces in TT. The matrix was heterogeneous: it consisted of an electron-dense component resembling phenolics and electron-transparent and fibrillar domains of various sizes (Figure 8A, Figure 8D–F, Figure 9A). The distance between TT cells (i.e., the enlarged intercellular spaces occupied by ECM) increased rapidly towards the center of the TT strand. Occasionally, pollen tubes were found in the matrix in styles from pollinated flowers (not shown).

4. Discussion

In rosaceans, stigmas of both wet and dry types were reported (Heslop-Harrison & Shivanna, 1977). However, stigmas of rosacean trees, in the few studies on *Malus* spp. or *Pyrus* spp., were classified as a wet type with a papillate surface and a moderate to slight amount of secretion present both on the stigma surface and in schizogenous intercellular cavities of the stigmatoid tissue distal portion, just below the papillate

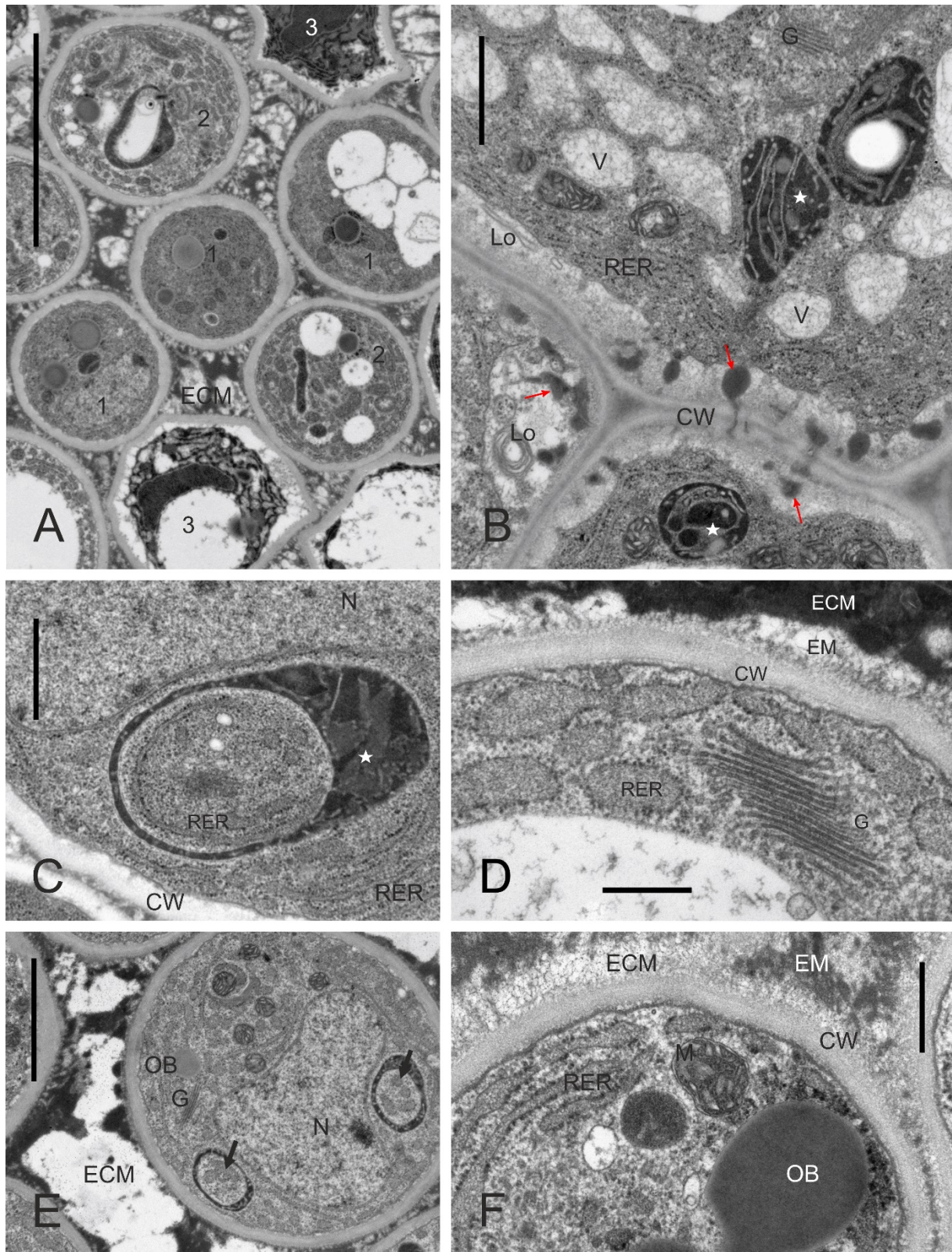


Figure 8 Ultrastructure of transmitting tissue, ‘Chojuro’, ‘Nijisseiki’, ‘Nijisseiki’, ‘Early Shu’, ‘Kosui’, ‘Shu Li’, respectively. (A) TT cells in different developmental stages: 1 – cells with narrow RER; 2 – cells with expanded RER containing fine fibrillar substance; 3 – degrading cells with expanded RER. (B,C) secretory activity and cup-shaped leucoplast with RER associated in stage 1 cells; (D–F) active Golgi, expanded RER, cup-shaped leucoplasts and a loosened outer face (vs. the inner one) of the cell wall in stage 2 cells. CW – cell wall; ECM – heterogeneous extracellular matrix; G – Golgi bodies; Lo – lomasomes; M – mitochondrion; N – cell nuclei; OB – oil bodies; RER – rough endoplasmic reticulum; V – vacuoles; asterisks – leucoplasts with extensive peripheral reticulum; slim red arrows – electron-dense substance in periplasmic space, thick arrows – RER in the concavity of cup-shaped leucoplasts. Scale bars 5 μm , 1 μm , 1 μm , 0.5 μm , 2 μm and 0.5 μm , respectively.

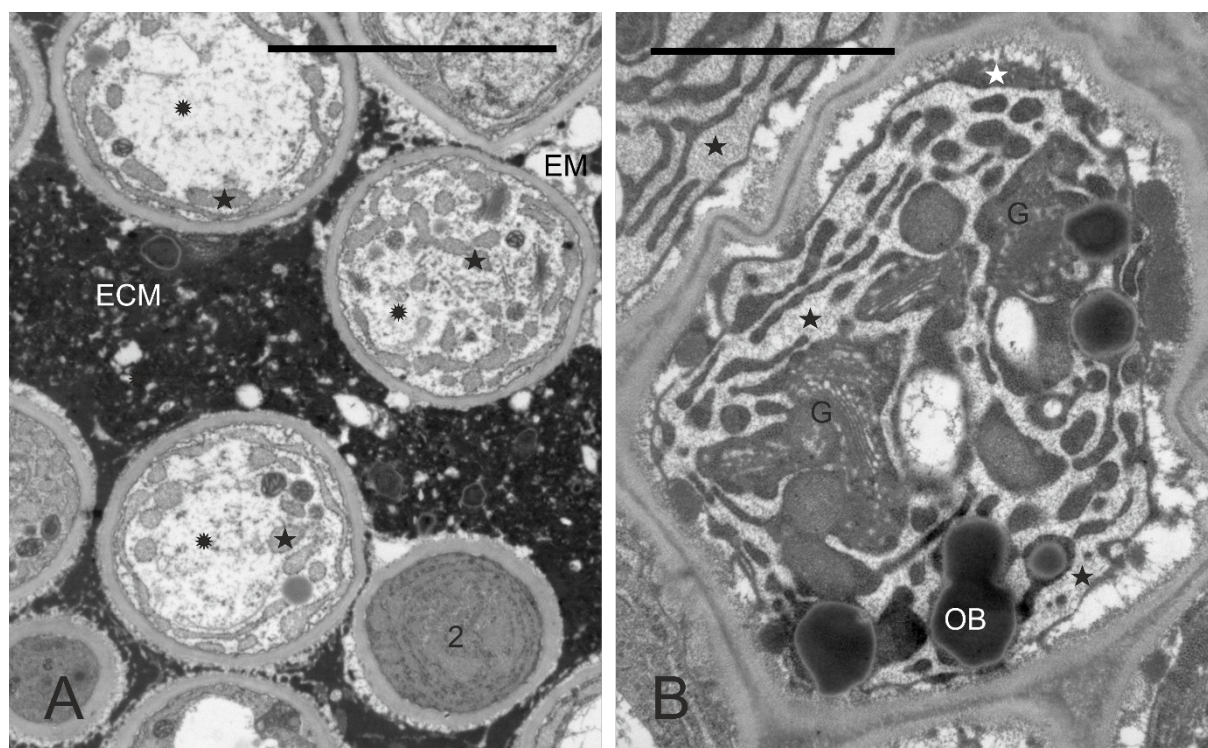


Figure 9 Ultrastructure of stage 3 transmitting tissue cells with electron-transparent cytoplasm undergoing lysis (rosettes in A) or electron-dense cytoplasm (white asterisks in B), ‘Early Shu’, ‘Shu Li’, respectively. ECM – heterogeneous extracellular matrix; G – Golgi bodies; OB – oil body; 2 – stage 2 cell with expanded RER; asterisks – lumen of expanded endoplasmic reticulum with fine-fibrillar substance. Scale bars 5 µm and 2 µm, respectively.

epidermis (Heslop-Harrison, 1976; Raghavan, 1997; Sanzol et al., 2003). The present study confirms these data.

To the best of our knowledge, the present work is the first report on the ultrastructure of the *Pyrus* spp. stigma. Generally, at the style and stigma boundary, a dramatic change occurs in the epidermis differentiation pathway. In the *Pyrus* taxa investigated here, as in most angiosperms, epidermal cells of the style and the stigma differ in every aspect of their ultrastructure, and the differences include cell shape and adherence to its neighbors, outer cell wall sculpture, cuticle thickness, its electron-density and striation, cytoplasm amount and vacuolation, endoplasmic reticulum-Golgi bodies-vesicles complex, and plastid ultrastructure. Concerning plastids, leucoplasts differentiate in both epidermal tissues of the *Pyrus* style in accordance with the high demand of these tissues for compounds typically produced by these plastids (mainly monoterpenes, e.g. Lange & Turner, 2012). However, the chemical components specific for the typical epidermal cell wall-cuticle complex differ from the secretion-cuticle complex of stigma exudate and, in our opinion, it is reflected in the different ultrastructure of leucoplasts in stylar epidermis and stigmatic papillae, as illustrated in the present study. Interestingly, the ultrastructure of leucoplasts observed in the stigmatic papillae (and in the TT cells) is compatible with the ultrastructure of these organelles typical for secretory cells in glandular hairs, secretory reservoirs etc. (e.g. Lange & Turner, 2012; Łotocka & Gęszprych, 2004). A significant difference is the absence of electron-dense globules or layer (possibly precursory compounds of the secretion) in the pear leucoplasts analyzed in the present study, in contrast to secretory leucoplasts documented in glandular trichomes or secretory epithelia (e.g. Ascensão & Pais, 1988; Cheniclet & Carde, 1988; Joel & Fahn, 1980; Mikulska & Żolnierowicz, 1976) or to tannosome-producing (underdeveloped) chloroplasts involved in the production of vacuolar proanthocyanidin inclusions (Brillouet et al., 2013).

In wet type stigmas, the secretion is supposed to overflow papillae through cuticle discontinuities. The stigmatic cuticle ultrastructure in *Pyrus*, with numerous folds and overlapping layers observed in this study, suggests “repair” of the cuticle at the

breaks. However, the formation of a “repair” layer does not require special secretory activity of the cells as it could result from aggregation of hydrophobic components of the secretion on its surface. As follows from the observations made during the present study, stigmatic epidermis differentiates into secretory cells, and this developmental pathway is also followed by the subepidermal cells of the stigma in contrast to the subepidermal parenchyma of the style. The striking ultrastructural resemblance of papillae and their subsurface neighbors (i.e., distal cells of stigmatoid tissue) indicate that they constitute a functional unit.

For the wet stigma, an experimental model is that of solanaceous genera (*Nicotiana*, *Lycopersicon*, *Datura*). Although Solanaceae (Asterid I clade) and Rosaceae (Rosid I clade) are rather remotely related, the ultrastructure of their stigmatic secretory cells is markedly similar (comp. the present study and data reported by Kandasamy & Kristen, 1987), which may be considered as a result of convergent adaptation to the same function.

As shown in the present study, at the same developmental stage of the *Pyrus* flower, another pistillar secretory tissue, TT of the style, had a markedly different ECM ultrastructure, cell wall, and protoplast components than the stigmatic secretory structures. The “secretion” of the stylar TT, the ECM, was very rich in electron-dense components, probably phenolics, in contrast to the secretion in the stigma. This is consistent with the general tendency of rosaceans to accumulate large amounts of phenolics (esp. tannins) in their tissues as an antimicrobial barrier (Maier et al., 2017). Both the stigma and the style are a potential infection gate for microbial pathogens. In agreement with the view by Raghavan (1997), the higher content of phenolics in TT ECM vs. stigmatic secretion seems logical, as the TT has a longer functional period during pollen tube penetration, and the style is not abscised in *Pyrus*. Transmitting tissue cells are thick-walled compared to stylar secretory cells, and the “dissolution” of the outer face of their walls is noticeable at anthesis. This suggests that the origin of the polysaccharide component of the ECM of TT is similar in the *Pyrus* spp. studied here, as in other species described in the literature: synthesis in Golgi bodies, exocytotic secretion *via* vesicles (both compartments abundantly present in TT cytoplasm), deposition in the cell wall and, finally, cell wall degradation. Interestingly, a similar way of a polysaccharide-rich ECM production through the degradation of outer cell wall layers occurs in specialized glands of some species that maintain symbiotic bacteria in leaf nodules (Lersten & Horner, 1967; Miller et al., 1983).

The most characteristic features of the TT protoplast ultrastructure noticed in this study are the prominent endoplasmic reticulum and numerous leucoplasts and their close spatial relationship with other organelles. Similar ultrastructure has been reported for *Malus communis* (Cresti et al., 1980) and Asiatic pear ‘Nijuseiki’ (Nakanishi et al., 1991), although in the latter species we do not confirm the presence of either that much periplasmic fibrillar secretion or fusion of vacuolar and periplasmic compartments. Interpretation of such an ultrastructure should be made in relation to the function of TT consisting in the secretion of components of the ECM, which generally include mostly carbohydrates (mainly pectins), amino acids, glycoproteins, glycolipids, and phenolic compounds, incl. tannins (Gotelli et al., 2017; Pereira et al., 2021) and inorganic components like exchangeable Ca^{2+} (Wasağ et al., 2018). Leucoplasts ultrastructurally similar to these observed in the present study are typical for both phenolic-secreting as well as terpenoid-secreting glandular trichomes and other secretory structures (Muravnik, 2021), which suggests their possible involvement in phenolic ECM component production and secretion in pear. Since the formation of tiny “droplets” resembling lipid bodies was often observed on the outer membrane of leucoplasts in the present study, it is possible that this indicates the secretion of a lipid precursor for glycolipid synthesis or membrane expansion (terpenoids are not reported to be present in the TT ECM). A prominent RER may be necessary to provide leucoplasts with proteins necessary for their biosynthetic pathways (in addition to supplying proteins to be secreted to the ECM). However, it is doubtful that the whole system of vastly expanded RER observed in this study contributed exclusively to the function of leucoplasts. Probably, after passage through prominent Golgi bodies, most of the RER-produced proteins were secreted to the

apoplast – e.g., the presence of large amounts of arabinogalactan proteins was reported for TT in multiple reports (e.g. Gane et al., 1994).

Generally, the results of our observations on the ultrastructure of TT in *P. pyrifolia* var. *culta* are consistent with those carried out by Nakanishi et al. (1991) on cv. Nijuseiki and with data on TT in *Malus* (Cresti et al., 1980). To our knowledge, the ultrastructure of TT in *P. communis* or the ultrastructure of the stigmatoid tissue in *Pyrus* spp. has not been studied earlier.

Acknowledgments

The Authors thank Ewa Znojek for her expert technical assistance. We thank anonymous Reviewers for their constructive criticism.

References

- Arber, A. (1937). The interpretation of the flower: A study of some aspects of morphological thought. *Biological Reviews*, 12, 157–184.
<https://doi.org/10.1111/j.1469-185X.1937.tb01227.x>
- Ascensão, L., & Pais, M. S. (1988). Ultrastructure and histochemistry of secretory ducts in *Artemisia campestris* ssp. *maritima* (Compositae). *Nordic Journal of Botany*, 8, 283–292.
<https://doi.org/10.1111/j.1756-1051.1988.tb01722.x>
- Bednarska, E. (1989). Localization of calcium on the stigma surface of *Ruscus aculeatus* L. *Planta*, 179, 11–16. <https://doi.org/10.1007/BF00395765>
- Bednarska, E. (1991). Calcium uptake from the stigma by germinating pollen in *Primula officinalis* L. and *Ruscus aculeatus* L. *Sexual Plant Reproduction*, 4, 36–38.
<https://doi.org/10.1007/BF00194569>
- Brillouet, J. M., Romieu, C., Schoefs, B., Solymosi, K., Cheynier, V., Fulcrand, H., Verdeil, J.-L., & Conéjéro, G. (2013). The tannosome is an organelle forming condensed tannins in the chlorophyllous organs of Tracheophyta. *Annals of Botany*, 112, 1003–1014.
<https://doi.org/10.1093/aob/mct168>
- Cheniclet, C., & Carde, J. P. (1988). Differentiation of leucoplasts: Comparative transition of proplastids to chloroplasts or leucoplasts in trichomes of *Stachys lanata* leaves. *Protoplasma*, 143, 74–83. <https://doi.org/10.1007/BF01282961>
- Claessen, H., Keulemans, W., Van de Poel, B., & De Storme, N. (2019). Finding a compatible partner: Self-incompatibility in European pear (*Pyrus communis*); molecular control, genetic determination, and impact on fertilization and fruit set. *Frontiers in Plant Science*, 10, Article 407. <https://doi.org/10.3389/fpls.2019.00407>
- Crawford, B. C., Ditta, G., & Yanofsky, M. F. (2007). The NTT gene is required for transmitting-tract development in carpels of *Arabidopsis thaliana*. *Current Biology*, 17, 1101–1108. <https://doi.org/10.1016/j.cub.2007.05.079>
- Crawford, B. C. W., & Yanofsky, M. F. (2008). The formation and function of the female reproductive tract in flowering plants. *Current Biology*, 18, R972–R978.
<https://doi.org/10.1016/j.cub.2008.08.010>
- Cresti, M., Ciampolini, F., & Sansavini, S. (1980). Ultrastructural and histochemical features of pistil of *Malus communis*: The stylar transmitting tissue. *Scientia Horticulturae*, 12, 327–338. [https://doi.org/10.1016/0304-4238\(80\)90047-3](https://doi.org/10.1016/0304-4238(80)90047-3)
- de Graaf, B. H. J., Derksen, J. W. M., & Mariani, C. (2001). Pollen and pistil in the progamic phase. *Sexual Plant Reproduction*, 14, 41–55. <https://doi.org/10.1007/s004970100091>
- Dumas, C., Rougier, M., Zandonella, P., Ciampolini, F., Cresti, M., & Pacini, E. (1978). The secretory stigma in *Lycopersicon peruvianum* Mill.: Ontogenesis and glandular activity. *Protoplasma*, 96, 173–187. <https://doi.org/10.1007/BF01279584>
- Edlund, A. F., Swanson, R., & Preuss, D. (2004). Pollen and stigma structure and function: The role of diversity in pollination. *The Plant Cell*, 16, S84–S97.
<https://doi.org/10.1105/tpc.015800>
- eFloras. (2008). *Flora of China*. Missouri Botanical Garden & Harvard University Herbaria. Retrieved November 25, 2022, from <http://www.efloras.org>
- Gane, A. M., Weinhandl, J. A., Bacic, A., & Harris, P. J. (1994). Histochemistry and composition of the cell walls of styles of *Nicotiana glauca* Link et Otto. *Planta*, 195, 217–225. <https://doi.org/10.1007/BF00199682>
- Gotelli, M. M., Lattar, E. C., Zini, L. M., & Galati, B. G. (2017). Style morphology and pollen tube pathway. *Plant Reproduction*, 30, 155–170.
<https://doi.org/10.1007/s00497-017-0312-3>
- Heslop-Harrison, J. (1976). A new look at pollination. *Annual Report of East Malling Research Station for 1975*, 141–157.

- Heslop-Harrison, Y., Heslop-Harrison, J., & Shivanna, K. R. (1981). Heterostyly in *Primula*. 1. Fine-structural and cytochemical features of the stigma and style in *Primula vulgaris* Huds. *Protoplasma*, 107, 171–187. <https://doi.org/10.1007/BF01275616>
- Heslop-Harrison, Y., & Shivanna, K. R. (1977). The receptive surface of the angiosperm stigma. *Annals of Botany*, 41, 1233–1258. <https://doi.org/10.1093/oxfordjournals.aob.a085414>
- Iketani, H., Katayama, H., Uematsu, C., Mase, N., Sato, Y., & Yamamoto, T. (2012). Genetic structure of East Asian cultivated pears (*Pyrus* spp.) and their reclassification in accordance with the nomenclature of cultivated plants. *Plant Systematics and Evolution*, 298, 1689–1700. <https://doi.org/10.1007/s00606-012-0670-0>
- Joel, D. M., & Fahn, A. (1980). Ultrastructure of the resin ducts of *Mangifera indica* L. (Anacardiaceae). 2. Resin secretion in the primary stem ducts. *Annals of Botany*, 46, 779–783. <https://doi.org/10.1093/oxfordjournals.aob.a085975>
- Kandasamy, M. K., & Kristen, U. (1987). Developmental aspects of ultrastructure, histochemistry and receptivity of the stigma of *Nicotiana glauca*. *Annals of Botany*, 60, 427–437. <https://doi.org/10.1093/oxfordjournals.aob.a087464>
- Lange, M. B., & Turner, G. W. (2012). Terpenoid biosynthesis in trichomes — current status and future opportunities. *Plant Biotechnology Journal*, 11, 2–22. <https://doi.org/10.1111/j.1467-7652.2012.00737.x>
- Lersten, N. R. (2008). *Flowering plant embryology: With emphasis on economic species*. John Wiley & Sons.
- Lersten, N. R., & Horner, H. T. (1967). Development and structure of bacterial leaf nodules in *Psychotria bacteriophila* Val. (Rubiaceae). *Journal of Bacteriology*, 94, 2027–2036. <https://doi.org/10.1128/jb.94.6.2027-2036.1967>
- Lolle, S. J., Berlyn, G. P., Engstrom, E. M., Krolikowski, K. A., Reiter, W. D., & Pruitt, R. E. (1997). Developmental regulation of cell interactions in the *Arabidopsis fiddlehead-1* mutant: A role for the epidermal cell wall and cuticle. *Developmental Biology*, 189, 311–321. <https://doi.org/10.1006/dbio.1997.8671>
- Łotocka, B., & Geszprych, A. (2004). Anatomy of the vegetative organs and secretory structures of *Rhaponticum carthamoides* (Asteraceae). *Botanical Journal of the Linnean Society*, 144, 207–233. <https://doi.org/10.1111/j.1095-8339.2003.00251.x>
- Łotocka, B., & Osińska, E. (2010). Shoot anatomy and secretory structures in several species of *Hypericum* (Hypericaceae). *Botanical Journal of the Linnean Society*, 163, 80–96. <https://doi.org/10.1111/j.1095-8339.2010.01046.x>
- Maier, M., Oelbermann, A. L., Renner, M., & Weidner, E. (2017). Screening of European medicinal herbs on their tannin content — New potential tanning agents for the leather industry. *Industrial Crops and Products*, 99, 19–26. <https://doi.org/10.1016/j.indcrop.2017.01.033>
- McGee-Russell, S. M. (1958). Histochemical methods for calcium. *Journal of Histochemistry and Cytochemistry*, 6, 22–42. <https://doi.org/10.1177/6.1.22>
- Mikulska, E., & Żołnierowicz, H. (1976). Ultrastructure of plastids in differentiating epithelial cells of *Abies homolepis* Sib. and Zucc. leaves. *Biochemie und Physiologie der Pflanzen*, 170, 355–362. [https://doi.org/10.1016/S0015-3796\(17\)30228-7](https://doi.org/10.1016/S0015-3796(17)30228-7)
- Miller, I. M., Gardner, I. C., & Scott, A. (1983). The development of marginal leaf nodules in *Ardisia crispa* (Thunb.) A.DG. (Myrsinaceae). *Botanical Journal of the Linnean Society*, 86, 237–252. <https://doi.org/10.1111/j.1095-8339.1983.tb00971.x>
- Muravnik, L. E. (2021). The structural peculiarities of the leaf glandular trichomes: A review. In K. G. Ramawat, H. M. Ekiert, & S. Goyal (Eds.), *Plant cell and tissue differentiation and secondary metabolites* (pp. 63–97). Springer Cham. https://doi.org/10.1007/978-3-030-30185-9_3
- Nakanishi, T. M., Saeki, N., Maeno, M., Ozaki, T., Kawai, Y., & Ichii, T. (1991). Ultrastructural study on the stylar transmitting tissue in Japanese pear. *Sexual Plant Reproduction*, 4, 95–103. <https://doi.org/10.1007/BF00196494>
- Pereira, A. M., Moreira, D., Coimbra, S., & Masiero, S. (2021). Paving the way for fertilization: The role of the transmitting tract. *International Journal of Molecular Sciences*, 22, Article 2603. <https://doi.org/10.3390/ijms22052603>
- Pitera, E., Molenda, E., & Odziemkowski, S. (2009). Prospects for cultivation of Asian pear in Poland. *Zeszyty Problemowe Postępów Nauk Rolniczych*, 536, 169–176.
- Pitera, E., & Odziemkowski, S. (2004). Evaluation of three Asian pear cultivars for cultivation in commercial orchards. *Journal of Fruit and Ornamental Plant Research*, 12, 83–88.
- Pruitt, R. E., Vielle-Calzada, J. P., Ploense, S. E., Grossniklaus, U., & Lolle, S. J. (2000). *FIDDLEHEAD*, a gene required to suppress epidermal cell interactions in *Arabidopsis*, encodes a putative lipid biosynthetic enzyme. *Proceedings of the National Academy of Sciences*, 97, 1311–1316. <https://doi.org/10.1073/pnas.97.3.1311>
- Raghavan, V. (1997). Stigma, style, and pollen-pistil interactions. In *Molecular embryology of flowering plants* (pp. 181–208). Cambridge University Press.

- Rejón, J. D., Delalande, F., Schaeffer-Reiss, C., Carapito, C., Zienkiewicz, K., de Dios Alché, J., Rodríguez-García, M. I., Van Dorsselaer, A., & Castro, A. J. (2013). Proteomics profiling reveals novel proteins and functions of the plant stigma exudate. *Journal of Experimental Botany*, 64, 5695–5705. <https://doi.org/10.1093/jxb/ert345>
- Sanzol, J., Rallo, P., & Herrero, M. (2003). Asynchronous development of stigmatic receptivity in the pear (*Pyrus communis*; Rosaceae) flower. *American Journal of Botany*, 90, 78–84. <https://doi.org/10.3732/ajb.90.1.78>
- Sheffield, C. S., Smith, R. F., & Kevan, P. G. (2005). Perfect syncarpy in apple (*Malus × domestica* ‘Summerland McIntosh’) and its implications for pollination, seed distribution and fruit production (Rosaceae: Maloideae). *Annals of Botany*, 95, 583–591. <https://doi.org/10.1093/aob/mci058>
- Wang, C. L., Wu, J., Xu, G. H., Gao, Y. B., Chen, G., Wu, J. Y., Wu, H. Q., & Zhang, S. L. (2010). S-RNase disrupts tip-localized reactive oxygen species and induces nuclear DNA degradation in incompatible pollen tubes of *Pyrus pyrifolia*. *Journal of Cell Sciences*, 123, 4301–4309. <https://doi.org/10.1242/jcs.075077>
- Wang, H., Wu, H. M., & Cheung, A. Y. (1996). Pollination induces mRNA poly (A) tail-shortening and cell deterioration in flower transmitting tissue. *The Plant Journal*, 9, 715–727. <https://doi.org/10.1046/j.1365-313X.1996.9050715.x>
- Wasąg, P., Suwińska, A., Zakrzewski, P., Walczewski, J., Lenartowski, R., & Lenartowska, M. (2018). Calreticulin localizes to plant intra/extracellular peripheries of highly specialized cells involved in pollen-pistil interactions. *Protoplasma*, 255, 57–67. <https://doi.org/10.1007/s00709-017-1134-8>